Journal of Environmental Management 296 (2021) 113090

Contents lists available at ScienceDirect

Journal of Environmental Management

journal homepage: www.elsevier.com/locate/jenvman

Impacts of historical ditching on peat volume and carbon in northern Minnesota USA peatlands

Liam Krause [a,1], Kevin J. McCullough [b], Evan S. Kane [a,d], Randall K. Kolka [c], Rodney A. Chimner [a], Erik A. Lilleskov [d,*]

[a] Michigan Technological University, 1400 Townsend Drive, Houghton, MI, 49931, USA
[b] USDA Forest Service, Northern Research Station, 1 Gifford Pinchot Dr., Madison, WI, 53726, USA
[c] USDA Forest Service, Northern Research Station, 1831 Hwy 169 E., Grand Rapids, MN, 55744, USA
[d] USDA Forest Service, Northern Research Station, 410 MacInnes Dr., Houghton, MI, 49931, USA

ARTICLE INFO

Keywords:
Minnesota peatlands
Ditching
Peat volume loss
Carbon emissions
GIS model
Wetland drainage

ABSTRACT

Peatlands play a critical role in terrestrial carbon (C) storage, containing an estimated 30% of global soil C, despite occupying only 3% of global land area. Historic management of peatlands has led to widespread degradation and loss of important ecosystem services, including C sequestration. Legacy drainage features in the peatlands of northern Minnesota, USA were studied to assess the volume of peat and the amount of C lost in the ~100 years since drainage. Using high-resolution Light Detection and Ranging (LiDAR) data, we measured elevation changes adjacent to legacy ditches to model pre-ditch surface elevations, which were used to calculate peat volume loss. We established relationships between volume loss and site characteristics from existing geographic information systems datasets and used those relationships to scale volume loss to all mapped peatland ditches in northern Minnesota (USA). We estimated that 0.165 ± 0.009 km^3 of peat have been lost along almost 4000 km of peatland ditches. Peat loss upslope of ditches was significantly less than downslope ($P < 0.001$). Mean width of the entire ditch-effect zone was 333 ± 8.32 m. Using our volume loss estimates, literature estimates of oxidation, and mean bulk density and peat C% values from Minnesota peatlands, we calculate a total historic loss 3.847 ± 0.364 Tg C. Assuming a constant oxidation rate during the 100 years since drainage, euic and dysic peatlands within the ditch effect zone have lost 0.26 ± 0.08 and 0.40 ± 0.13 Mg C ha^{-1} yr^{-1}, respectively, comparable to IPCC estimates. Our spatially-explicit peat loss estimates could be incorporated into decision support tools to inform management decisions regarding peatland C and other ecosystem services.

1. Introduction

Carbon (C) retention in natural landscapes is widely recognized for its role in regulating greenhouse gases (GHG). Among the "natural climate solutions" identified as potential approaches land managers can adopt to support GHG emissions reduction goals, two are focused on peatlands: the avoidance of impacts on peatlands and, where disturbance has occurred, active peatland restoration (Griscom et al., 2017).

The reason for this focus is simple: although peatlands represent only ~3% of terrestrial land area (Xu et al., 2018), during the Holocene they accumulated ~30% of the organic C found in global soils (Page and Baird, 2016), meaning they are massive C sinks on millennial timescales. However, land use changes in peatlands impact their C storage capacity (Loisel et al., 2020). Peatland drainage to facilitate agricultural and agroforestry production in saturated soils has impacted over 65 million ha worldwide (Kaat and Joosten, 2008). Drainage precipitates changes in biogeochemical processes that regulate long-term C storage (Drexler et al., 2009), converting impacted peatland ecosystems from net C sinks to sources. Without intervention, it is estimated that by 2100, CO_2 emissions from degraded global peatlands will account for 12–41% of the remaining global CO_2 emissions budget required to keep global warming under the 1.5–2 °C threshold (Leifeld et al., 2019).

In Minnesota, saturated soils within the state's ~24,000 km^2 peatland area (MNDNR, 1984), which represent around 12% of the entire

* Corresponding author.
E-mail addresses: lmkrause@mtu.edu (L. Krause), Kevin.McCullough@usda.gov (K.J. McCullough), eskane@mtu.edu (E.S. Kane), Randall.K.Kolka@usda.gov (R.K. Kolka), erik.a.lilleskov@usda.gov (E.A. Lilleskov).
[1] USDA Forest Service, Eastern Region Regional Office, 626 E. Wisconsin Ave., Milwaukee, WI, 53202 USA (Liam Krause permanent address).

https://doi.org/10.1016/j.jenvman.2021.113090
Received 13 February 2021; Received in revised form 11 June 2021; Accepted 13 June 2021
Available online 10 July 2021
0301-4797/© 2021 Published by Elsevier Ltd.

peatland area in the United States (Xu et al., 2018), have experienced extensive ditching and degradation. Systematic drainage in Minnesota peaked between 1900 and 1920 (Wilson, 2016) and, although new peatland drainage is infrequent in Minnesota today, the legacy of historic drainage during the 19th and 20th-centuries can be seen in a gridded ditch network that patterns the state's northern counties (Figure S1). It is estimated that over 33,000 km of surface drainage ditches and channelized waterways have been installed across the state (Hanson, 1987).

While these ditching projects largely failed to facilitate agricultural production (Bradof, 1992), they have a continued effect on the structure and function of the peatland landscape (Gorham and Wright, 1979). Ditches alter peatland hydrology, increasing air-filled pore-space in the upper strata of the peat matrix, in turn promoting rapid decomposition rates of the organic peat material with the onset of aerobic microbial processing (Clymo, 1983). The removal of water from the pores in the peat matrix also initiates compaction associated with the decreased buoyancy of the acrotelm (Hooijer et al., 2012). The effect of these chemical and physical changes results in land subsidence.

Peatland response to drainage is influenced by peatland soil structure and the hydraulic conductivity of the peat matrix (Boelter, 1972), peatland slope (Stewart and Lance, 1991), degree of humification of peat material (Boelter, 1968), ditch orientation, and climatic conditions (Braekke, 1983). How peatland ecosystems respond to drainage can differ based on the extent to which they are hydrologically connected to groundwater sources (Moore and Bellamy, 1974). Minnesota has a gradient of peatlands from bogs to poor-, intermediate-, and rich fens. Ombrotrophic bogs are hydrologically isolated from groundwater, receiving most of their moisture and mineral inputs from precipitation. Their soils are acidic and contain poorly-humified peat, supporting vegetation communities dominated by *Sphagnum* mosses, ericaceous shrubs, and black spruce (*Picea mariana*). At the other end of the nutrient gradient are minerotrophic fens, which are characterized by hydrologic connectivity with base-rich groundwater, leaving them more nutrient rich and alkaline than bogs. These peatlands tend to support higher productivity graminoid plant communities and contain more highly humified peat material (Bridgham et al., 1998).

The bulk density and degree of humification of the two broad peatland types influence potential subsidence. Bog peat, comprised primarily of recalcitrant *Sphagnum* material, is generally less-well decomposed, less dense, and has larger pore spaces than fen peat (Minkkinen and Laine, 1998; Bridgham et al., 1998; Hill et al., 2016). Mechanical settling of peat during subsidence is greater in a matrix with larger pore sizes. Additionally, lower bulk density permits greater saturated hydraulic conductivity (Rezanezhad et al., 2016). Thus, ditch effectiveness increases with the decrease in the bulk density of surface peat (Boelter, 1972). The slope and position of the ditch on the landscape also affects ditch effectiveness, e.g., affecting its ability to capture upslope runoff, isolating the downslope side of the ditch from water inputs (Stewart and Lance, 1991).

Our goal was to assess the historical impact of legacy drainage ditches on the peatlands of northern Minnesota. Our investigation of the distribution of degraded peatlands and the characteristics that help predict volume and C loss will further assist in the prioritization of restoration activities, especially within the scope of natural climate solutions strategies.

We hypothesized that: 1) humified peat will reveal a less pronounced peat loss response to ditching than acidic, fibric peat; 2) peat loss will exhibit a dependent relationship with landscape and climatic variables; 3) the downslope side of a ditch will experience more peat loss than the upslope side of a ditch. Ultimately, we develop a spatially explicit estimate of the amount of C loss as a result of peatland ditching in northern Minnesota.

2. Materials and methods

2.1. Study area

The study was conducted in two ecological provinces within northern Minnesota: the Laurentian Mixed Forest Province and the Tallgrass Aspen Parklands Province (MNDNR, 2003; MNDNR, 2005a). We excluded two of Minnesota's ecological provinces, the Prairie Parklands and Eastern Broadleaf Forest Provinces. Whereas peatlands cover ~21% of the combined area of the Laurentian Mixed Forest and the Tallgrass Aspen Parklands provinces, lower initial peatland density combined with land use changes following European settlement result in a much smaller area of peat-forming ecosystems in the Prairie Parklands and Eastern Broadleaf Provinces (MNDNR, 2005a, MNDNR, 2005b, see also Supplementary Materials, S1).

Ditching in the study area occurred primarily during the early 20th century (MNDNR, 1987), starting in 1897 with the creation of a state drainage commission and continuing into the 1920s (Averell and McGrew, 1929; Hanson, 1987; Bradof, 1992). Most of the ditches were dug to depths of 1–2 m (Averell and McGrew, 1929). Widths at the top of the ditches generally ranged from 3.5 to 6 m, while the width at the bottom of the channel was 1–3 m (Averell and McGrew, 1929). Ditch spacing varied by location, but generally adopted a gridded configuration and was often found to be ~1600 m by 1600 m (1 × 1 mile) or 1600 m by 3200 m (Averell and McGrew, 1929; MNDNR, 2016). General, although not universal, practice at the time of installation was to place the excavation spoils on the downflow side of the ditch to facilitate the natural flow of upslope water into the ditch (Averell and McGrew, 1929). Most peatland ditches in northern Minnesota have not been maintained regularly since installation (Averell and McGrew, 1929; Bradof, 1992).

2.2. Site selection

All geospatial analyses were conducted in Arc Pro 2.5.1 and ArcGIS Desktop 10.8.1. To generate an estimate of peatland distribution within the two ecological provinces, we used data from the updated Minnesota NWI (MNDNR, 2019) and the Soil Survey Geographic (SSURGO) database (SSURGO, 2019). From SSURGO, we extracted all polygons in which at least 85% of the polygon area was classified with the taxonomic soil order Histosol (classified as a soil with a surface organic layer depth over 40 cm (Kolka et al., 2016)). We classified as peatlands all of this Histosol area that was also classified as wetlands from the NWI, irrespective of whether peat was indicated in the NWI wetland classification. The intersection of the SSURGO Histosol and NWI layers included 86% (12,143 km^2) of the area of all NWI features classified with coding for peatlands in the study area (see also Supplementary Materials, S2). All data used in this analysis were projected to the NAD 83 UTM zone 15 N.

We used the Minnesota Buffer Protection layer (MNDNR, 2016) to delineate the locations of ditches in the study area. We calculated an intersection of the Public Ditch features with the peatland layer described above for a total estimate of public ditches that exist within peatlands in the study area.

We used the MNDNR NWI Wetland Finder (Kloiber et al., 2019) and the MNDNR topography tool, MN TOPO (MNDNR, 2014), to examine summer imagery and contour lines across the ditch network to select 69 sites for pre-ditch surface estimation based on visual estimations of the surrounding continuity of the peatland. This was done to avoid the confounding influence of topographic variation caused by interspersed upland features on our pre-ditch surface estimation model. Fourteen sites are controls with no ditches present (hereafter referred to as "Control"), 33 are single ditch sites (hereafter "Across"), and 22 sites have two ditches that intersect (hereafter "4-corner").

We accessed LiDAR elevation data from the MnGeo FTP server. Statewide LiDAR data were collected at a 1 m horizontal resolution

between 2005 and 2012 by MNDNR and Woolpert, Inc. (MNDNR, 2017).

For each site identified, we established a site center point. In the case of Across site types, site center points were established on the centerline of a single ditch, avoiding areas with adjacent upland features. Four-corner site center points were placed in the middle of the intersection of two intersecting ditches. Control site center points were placed in larger unditched peatland areas.

Analysis of elevation change in this study employed methods similar to those in Williamson et al. (2017), though with the goal of developing spatially explicit predictions of volume loss along a ditch network using site characteristics. Our analysis utilized two separate measures of elevation change along the ditch network. The first (transect) approach uses 1 m LiDAR elevation data to model pre-ditch surfaces using the elevation profile of a 1000 m linear feature drawn perpendicular to the ditch. The second (surface trend) approach uses 1 m LiDAR elevation data to model a surface trend over an area of interest (AOI) and was used as an alternative approach (described in Supplementary Materials, S4).

For the transect approach in the Across sites, four 1000 m transects were established perpendicular to the single ditch (Fig. 1). Where possible, the two transects on either end were placed midway between the site center point and a ditch junction or ditch endpoint. The inner Across site transects were evenly positioned about the site center point between the two end transects. This spacing was approximately 450 m, unless upland features did not permit uniform spacing, in which case placement was adjusted to avoid upland features while attempting to maintain a uniform spacing. In the 4-corner sites, four 1000 m transects were established on each intersecting ditch, two on each of the four arms of the ditch intersection, for a total of eight transects per 4-corner site. Each of these eight transects was placed perpendicular to the respective ditch segment with 500 m extending out on either side. The four outermost transects were placed approximately at the midpoint between the site center point in the ditch intersection and the adjacent ditch intersection midpoint. The four innermost transects were located midway between the site center point and the outer transect. Because some sites were immediately adjacent to each other in a gridded ditch formation, 14 transects found at the midpoints between two sites were not duplicated and are shared between sites. Because the surface trend analysis required a larger area of continuous landscape uniformity than does the transect approach, it was not possible to perform this process on all 69 sites. We therefore conducted the surface trend analysis on 38 sites, (14 control, 5 Across, and 19 4-corner), for comparison with the transect approach.

AOI sizes for each site were determined by the distance between the center point location of each site and the midpoint between the site center point and any adjacent ditch intersections. It was necessary to restrict the size of the AOI to isolate the effect of a single ditch while excluding the potential elevation change generated by neighboring ditches. If distance between ditch intersections was at least 1500 m, 1500 × 1500 m was used as the default site dimension, otherwise sizes were reduced to 1000 × 1000 m. Twelve sites were assigned a size of 1000 × 1000 m, while the remaining 57 sites were assigned 1500 × 1500 m.

2.3. Analysis of elevation change

2.3.1. Transect approach

Using 3D Analyst tools and 1 m LiDAR data in ArcGIS, an elevation profile was created by plotting elevation vs. distance on a scatterplot for each transect. We plotted and inspected each elevation profile to determine a point on either side of the ditch midpoint that deviated from the trend of the surrounding landscape (Fig. 1). The area between the two deviation points is referred to as the ditch effect zone. Using only the elevation data from beyond the ditch effect zone, we tested linear, second-order, and third-order polynomial fits of a line to model the pre-ditch elevation above the ditch effect zone.

Using the regression equation output from the modeled fit of the line, we found the predicted elevation value for all points within the ditch effect zone. To calculate total volume change along the length of a transect, we subtracted the observed elevation value from the predicted pre-ditch elevation value. These differences were summed for a total volume change estimate for each transect, which represents the total volume change given 1 m of ditch length. Given the similarity between the values measured with the three tests (Table 1); the dominance of concave or convex land surfaces, i. e, with only one inflection point (e.g., Fig. 1); and the convention of using the lowest-order polynomial fit to limit bias, we chose the second-order polynomial fit of a line to estimate all volume change with the transect method.

Table 1
Mean ± SE volume change per meter of ditch length for both transect and surface trend methods using linear, second- and third-order polynomial fits.

Fit Method	Transect (m^3) n = 294	Surface Trend (m^3) n = 24
Linear	59.69 ± 3.09	62.50 ± 9.17
Second-order polynomial	59.80 ± 2.95	56.47 ± 7.06
Third-order polynomial	58.93 ± 2.94	56.46 ± 7.02

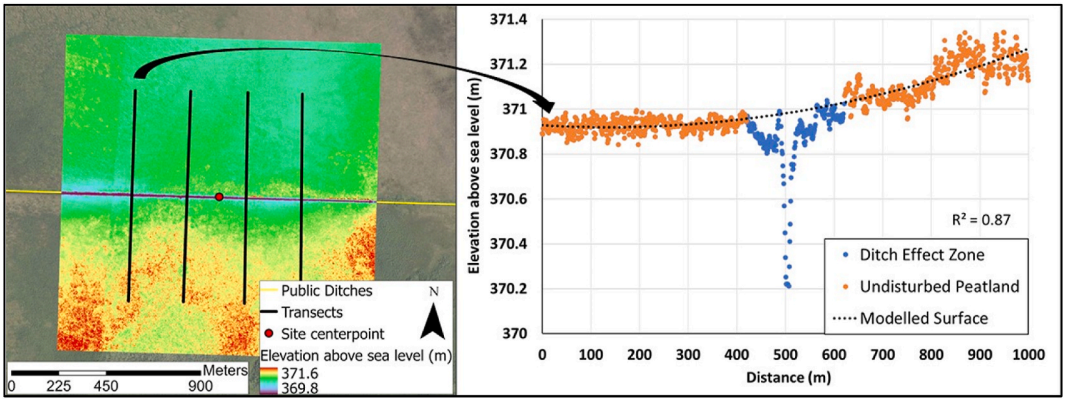

Fig. 1. Transect approach. Four 1000 m transects are centered perpendicular to each ditch within an Across (single ditch) site AOI. From 1 m elevation data, elevation profiles of the ditch were created. A second-order polynomial fit of a line is fit to the elevation points from the undisturbed distal segments (orange points) of the transect. Using the line of best fit, volume change is calculated by subtracting the elevation data of the "ditch effect zone" (blue points) from the elevation of the modeled surface. (Graphic created in Arc Pro 2.5.1 and Microsoft Excel, 2019. Elevation data was obtained from the Minnesota Geospatial Commons and manipulated. Composite aerial imagery and ditch layers obtained from the Minnesota Geospatial Commons with full attribution in Supplementary Materials, S11). (For interpretation of the references to color in this figure legend, the reader is referred to the Web version of this article.)

2.4. Analysis of wetland type

To assess any relationship between total volume change along the elevation profile transects and wetland type, we used GIS layers describing wetland type, and soil characteristics. To assign Cowardin wetland classes to each transect, we intersected transects with the updated Minnesota NWI, and then assigned to each transect the Cowardin "class" that intersected with >50% of the length beyond the ditch effect zone (>150 m on either side of the ditch), reflecting pre-ditch peatland classes. These were either FO, SS, or EM representing a forested, scrub/shrub or emergent class in a Palustrine system, respectively (Kloiber et al., 2019).

We conducted a similar process to intersect each transect with the SSURGO data to identify the soil taxonomic suborder and the carbonate reaction class. Each transect was assigned the taxonomic suborder and carbonate reaction class (SSURGO, 2019) that intersected with >50% of the length beyond the ditch effect zone. The Histosol taxonomic suborders found in the study area describe a gradient of organic material humification, i.e., sapric > hemic > fibric. The carbonate reaction class relates to the pH level within a soil polygon, i.e., dysic (<4.5) and euic (≥4.5). These classifications were used as broad estimates of ombrotrophic and less minerotrophic (dysic) vs. more minerotrophic (euic) peat types.

2.5. Analysis of climatic and slope attributes

At each transect center point, we extracted mean annual temperature (MAT) and mean annual precipitation (MAP) data from the PRISM dataset (PRISM, 2019). These data were accessed at a spatial resolution of approximately 800 m. We also extracted data describing mean annual actual evapotranspiration (AET) and the Priestley-Taylor Alpha Coefficient, which describes the ratio of AET over potential evapotranspiration, at a 30 arc-second resolution from Trabucco and Zomer (2019). Slope characteristics at the midpoint of each transect, derived from the slope geoprocessing tool, were extracted using 10 m elevation data.

2.6. Statistical analysis

We performed all data analyses in the statistical programming environment R (R Core Team, 2020). To determine which factors from the transect-level data were predictive of peat volume loss and could be used to scale to the map level, we implemented multi-level unbiased recursive partitioning (Hothorn et al., 2006; Fokkema et al., 2018) through the R package glmertree (Fokkema et al., 2020) to create a generalized linear mixed-model (GLMM) tree of peat volume change.

In our GLMM tree, we used a restricted maximum likelihood estimation of a random intercept for the transect site and of the following fixed effect parameters: soil taxonomic suborder, carbonate reaction, NWI Cowardin class, slope degree, PRISM MAT and MAP, AET, and the Priestley-Taylor coefficient. Variable selection parameters were set at $\alpha = 0.05$ with Bonferroni-corrected p values and a minimum node size of 40 observations. This conservative method prevented potential overfits of the GLMM tree model (see also Supplementary Materials, S5, S6).

We investigated the predictive capabilities of the GLMM tree model by classifying all ditches within the entire study area, including AOIs, using the three predictor variables from the terminal nodes of the GLMM tree. SSURGO carbonate reaction class was applied to ditch segments by first generating 1000 m transects orthogonal to the ditch at 5 m intervals along its entire length. Each of these transects was assigned the majority reaction class that intersected with the segment of the transect beyond the ditch effect zone (150 m on either side of the ditch). The reaction class for each transect was used to determine the reaction class assigned to its respective 5 m ditch segment. Slope derived from 10 m elevation data and MAP data were intersected with the location of the ditch. We then compared our volume loss predictions from GLMM tree ditch classifications with the AOI volume loss observations from both transect and surface trend analyses. Within each AOI, we multiplied the length of each GLMM tree ditch classification by the median volume loss value reflected in each classification's respective terminal node. We summed the volume loss values returned by this approach within each site AOI for a predicted areal estimate of volume change and regressed those values against volume change observed with the surface trend analysis. The same ditch classification approach described above was adopted to scale volume change estimates to the entire study area. A map that includes the peatland area and GLMM tree-classified ditches can be found in the Supplementary Materials (Supplementary Materials, S9).

2.7. C loss analysis

To estimate C loss represented by volume loss, we used an equation predicting relative contribution of oxidation to subsidence from years since drainage, described in Pronger et al. (2014):

$$\%\ \text{oxidation} = 13.4 * \text{yr}^{0.29} \quad (1)$$

This predicted that the percent of subsidence attributable to oxidation was 51% ± 7.83 (mean ± se). We used two different datasets to obtain average bulk density values for both euic and dysic peat types, both collected from various locations in Minnesota. The first dataset contains averaged peatland bulk density values from within the top 25 cm of peat reported in Bridgham et al. (1998), from which we excluded the observations of one mineral site type. From the second dataset, we averaged peatland bulk density values from the 35–50 cm depth collected as part of a statewide peat inventory from Minnesota peatlands (MNDNR, 2007), excluding samples that were missing data or were taken within 200 m of a ditch. Observations from both datasets were separated by pH value into dysic and euic classes and the bulk density values were averaged for 0.09 ± 0.003 g cm^{-3} and 0.13 ± 0.004 g cm^{-3} for dysic and euic, respectively. These estimates are similar to other Minnesota peat bulk density measurements described in the literature (Boelter, 1968). The estimated fractional C content of the peat dry mass used was 0.426 ± 0.004 and 0.424 ± 0.016 for dysic and euic, respectively (Bridgham et al., 1998). Total C loss for each ditch classification based on GLMM tree nodes was then estimated using the following equation:

$$\text{Mg C loss} = \text{m}^3\ \text{peat volume} * \text{bulk density}\left(\text{Mg/m}^3\right) * \text{fraction oxidized (unitless)} * \text{fractional C content (unitless)}. \quad (2)$$

To estimate C losses per hectare per year, we first calculated area affected for each terminal node in the tree:

$$\text{ha affected} = \text{km ditch length} * \text{km ditch width} * \left(100\ \text{ha/km}^2\right) \quad (3)$$

For ditch length, we used total ditch length for each GLMM tree node. For ditch width, we used average ditch effect width for each node based on the transect data. We then divided the total historic C loss values as described above by disturbed area and total elapsed time using the following equation:

$$\text{Mg C ha}^{-1}\ \text{yr}^{-1} = (\text{Mg C loss} / \text{ha affected})/100\ \text{yr} \quad (4)$$

We used 100 years as the time elapsed since drainage based on the difference between the central value of 1908 for drainage (because most of the peatland drainage in northern Minnesota occurred between 1897 and 1920 (Averell and McGrew, 1929; Hanson, 1987; Bradof, 1992)), and the central value for LiDAR of 2008 (since LiDAR data were collected between 2005 and 2012 (MNDNR, 2017)).

3. Results

3.1. Peatland area and ditch length

The calculated peatland area in the two ecological provinces is 22,105 km^2. Subdivided by soil taxonomic suborder, 445 km^2 were classified as fibrists, 12,382 km^2 were classified as hemists, and 9278 km^2 were classified as saprists (Supplementary Materials, Table S2, S3). Classifying by SSURGO carbonate reaction class (dysic < 4.5 pH, euic ≥ 4.5 pH), 6671 km^2 were classified as dysic and 15,254 km^2 were classified as euic (180 km^2, or 1% of the peatland area, had no designation). Ninety-eight percent of the peatland area was classified in the Minnesota NWI by three Cowardin classes: forested wetlands (9273 km^2), scrub/shrub (8532 km^2), and persistent emergent (3963 km^2). Total ditch length within the study peatlands was 3948 km.

3.2. Observed volume change

3.2.1. Transect approach

Mean volume change (±SE) across all ditched peat transects measured using a second-order polynomial fit of a line (n = 294) was 59.80 ± 2.95 m^3 per meter of ditch length. Mean volume change for control sites was not significantly different from zero, i.e., 1.16 ± 1.23 m^3 per transect (n = 56). Mean R^2 of the line fitted to elevation data from the undisturbed segments of the transect was 0.78 ± 0.01. This value is slightly depressed given that so many of our sites were at near-zero surface slope, which result in poor R^2 despite a good fit to a line. Volume loss values estimated by the three best fit methods were comparable (Table 1). In support of hypothesis 3, ditch-effect width and volume loss were both larger on the downslope side of the ditch ($P < 0.001$; Table 2). Mean width of the ditch effect zone was 333 ± 8.32 m.

3.2.2. Transect vs. surface trend approach

In ditched sites, there was a positive relationship between the volume change measured using the surface trend approach and the transect approaches ($R^2 = 0.70$, $P < 0.001$). Using the surface trend approach, mean volume loss in control sites was 0.001 ± 0.003 $m^3\ m^{-2}$ in each AOI.

Standardizing surface trend analysis volume change measurements by meter ditch length within the AOI led to a volume loss of 56.46 ± 7.02 m^3 per-meter ditch length (Table 1). While mean per-meter volume loss is similar between the two methods, there was a small but significant difference ($P < 0.005$) between the transect (2nd order polynomial) and surface trend modeling (3rd order polynomial) approaches (Table 1).

3.3. Volume change relationship to site characteristics

In support of our first hypothesis, soil carbonate reaction class, soil taxonomic suborder, and the Cowardin class all exhibited significant relationships with peat loss (Fig. 2). The more acidic, lower bulk density ombrotrophic *Sphagnum* peatland types with the dysic designation exhibited more loss than did the higher pH minerotrophic peatlands.

Five continuous variables had a positive relationship with volume loss: ditch slope degree ($R^2 = 0.15$, $P < 0.001$), MAP ($R^2 = 0.15$, $P < 0.001$), MAT ($R^2 = 0.03$, $P = 0.003$), AET ($R^2 = 0.14$, $P < 0.001$), and the Priestley-Taylor Alpha Coefficient ($R^2 = 0.16$, $P < 0.001$) (Table S1). This supports our second hypothesis that peat volume loss would be dependent on landscape and climatic variables.

Table 2
Volume change and ditch effect width ± SE measured on both the upslope and downslope side of the ditch. Paired t-tests between upslope vs. downslope width and volume change were both significant ($P < 0.001$).

Characteristic	Mean ± se	Min	Max
Downslope ditch effect width (m)	190.88 ± 5.85	9	410.59
Upslope ditch effect width (m)	142.15 ± 4.90	2	411.37
Downslope volume change (m^3)	34.18 ± 1.85	−13.16	212.75
Upslope volume change (m^3)	25.78 ± 1.48	−22.21	142.72

Table 3
Volume change per meter of ditch length ± standard error of the mean from each category as classified by terminal nodes of GLMM tree. Ditch length is the length of ditch within the study area, classified by terminal nodes of GLMM tree.

GLMM tree node	Mean ± se (m^3)	Median (m^3)	Ditch length (km)
Node 4 - Dysic, low slope, low MAP	60.89 ± 4.88	55.52	568.47
Node 5 - Dysic, low slope, high MAP	87.78 ± 5.77	78.75	357.8
Node 6 - Dysic, high slope	120.08 ± 9.90	106.01	328.79
Node 8 - Euic, low slope	24.86 ± 2.60	17.42	1479.53
Node 9 - Euic, high slope	48.24 ± 5.01	36.78	1213.15

3.4. Volume change predictions

The recursive partitioning analysis selected one categorical variable and two continuous variables (Fig. 3). Soil carbonate reaction class was the most significant partitioning variable ($P < 0.001$), followed by slope degree ($P < 0.001$). At both nodes in the tree where slope was the variable selected, the higher slope node showed higher volume loss. A final split of node three was selected using MAP as a partitioning variable ($P = 0.045$). Volume loss was higher in the high precipitation node than the low precipitation node. The resulting tree displays the volume loss per meter of ditch length based on transect-level characteristics, classified into five terminal nodes (Fig. 3).

Predicted volume change values within each site based on the classification of each ditch by the GLMM tree nodes also demonstrated a strong relationship with transect averages from each AOI, scaled to AOI by ditch length ($R^2 = 0.74$) (Fig. 4a). There was also a positive relationship between predicted values and volume change values measured using the surface trend method ($R^2 = 0.62$) (Fig. 4b).

3.5. Total peat volume and carbon loss estimations

Total calculated peat volume loss associated with the ditches is 165.3 million ±8.6 million m^3 (Fig. 5). Despite making up only 32% of ditch length, dysic-classified ditches account for 57% of total volume loss.

Total calculated historic C loss was 3.85 ± 0.36 Tg C. Due to higher average bulk densities, the proportion of C loss to volume loss is higher in euic than in dysic types, although the elevated volume loss per unit area from dysic types outweighs this, so C losses per meter ditch length and per unit area are highest in dysic types (Table 4, Table 5).

4. Discussion

We used a novel approach to identify specific predictors of peatland C loss that could be scaled using GIS methods, providing spatially explicit estimates of peat volume and C loss across northern Minnesota. Peat losses across the region were substantial, and were predicted by a suite of variables suitable for scaling using GIS, permitting estimates of regional peat and C loss. Although there are uncertainties in our calculations, the findings converge with estimates of boreal peatland C loss developed using other site-level analysis methods.

4.1. Peat loss magnitude and comparison with literature emissions factors

To make decisions about the benefit of peatland restoration vs. other interventions, it is important to understand the potential long-term and current magnitude of emissions of C and CO_2 from these drained peatland ecosystems. The total calculated historic loss of ~0.165 km^3 of peat

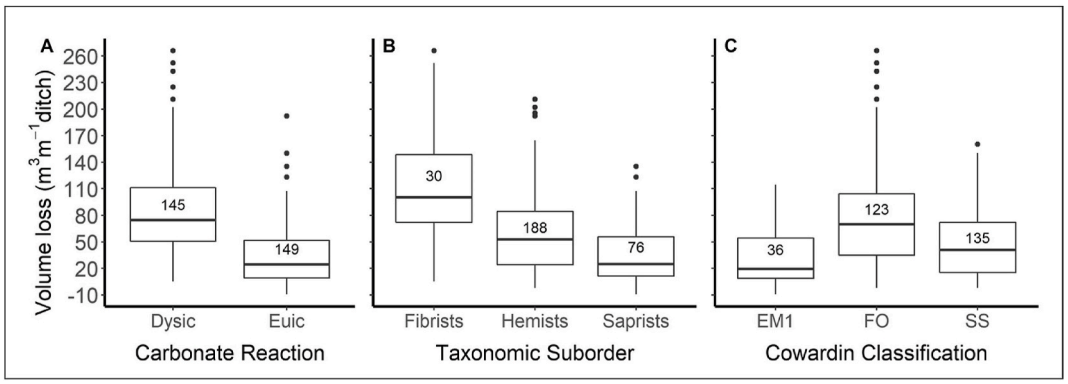

Fig. 2. Volume change per meter ditch length by soil and wetland characteristics (n = 294). EM1 = persistent emergent, FO = forested, SS = scrub/shrub.

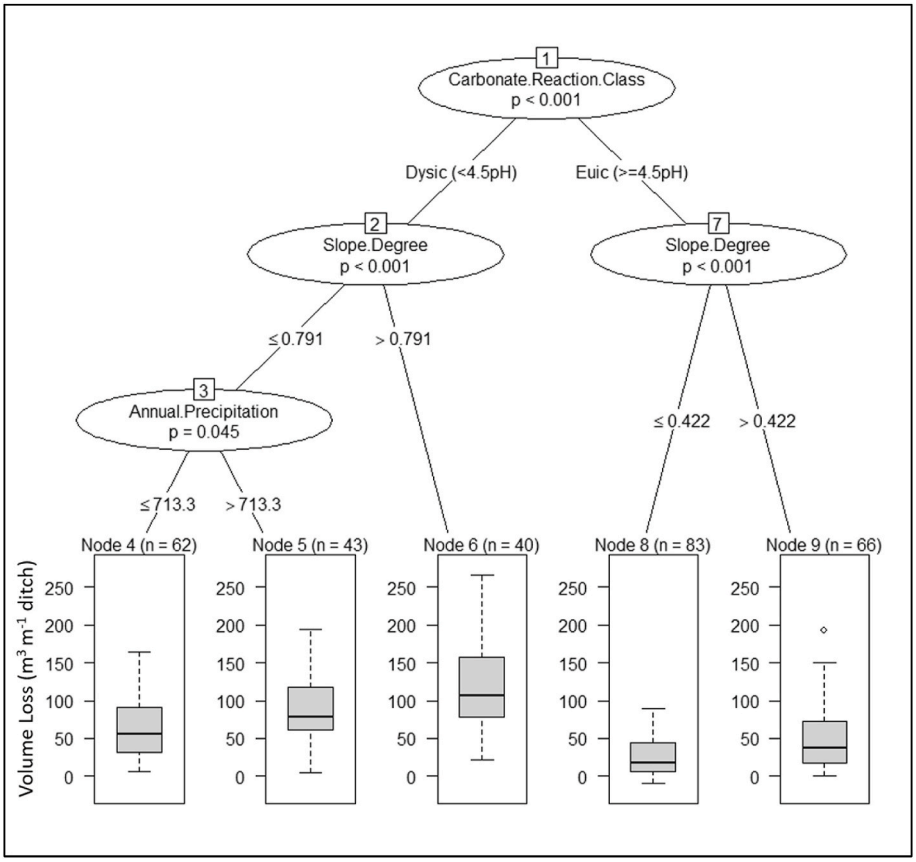

Fig. 3. Volume change values classified by site characteristics as determined using multi-level unbiased recursive partitioning. The y-axis in each terminal node represents the volume change in $m^3\ m^{-1}$ of ditch length (also see Table 3). Carbonate reaction class is from the SSURGO dataset, slope degree is derived from 10 m resolution elevation data, and MAP is from the PRISM dataset.

in this study area translated to estimated C emissions of ~3.85 Tg C, roughly equivalent to 0.05% of the total calculated peatland C pool in the conterminous United States (Kolka et al., 2018).

Assuming a constant emissions rate over 100 years, the above estimate of total C loss translates to 0.0385 Tg C yr^{-1}, or 0.141 Tg CO_2-eq yr^{-1}, which is approximately 0.09% of annual emissions from all sectors in Minnesota in 2016 (Minnesota Pollution Control Agency, 2019). This estimate is conservative, as it does not cover 100% of peatland area in the state, nor does it account for the fact that intact peatlands have a net uptake of CO_2. The latter can be accounted for as follows. Long-term rates of C accumulation in Minnesota peatlands are ~0.26 Mg C ha^{-1} yr^{-1}, or 0.96 Mg CO_2-eq ha^{-1} yr^{-1} (Gorham et al., 2003; McFarlane et al., 2018). Scaled up over the entire ditch affected area, this is ~0.032 Tg C yr^{-1}, or about equal to the annual average loss term that we calculated. Combining our loss estimate (0.0385 Tg C yr^{-1}) with this long-term accumulation rate (0.032 Tg C yr^{-1}), the difference in fluxes between the current loss from ditched areas and long-term accumulation rates is ~0.071 Tg C yr^{-1} (~0.259 Tg CO_2-eq yr^{-1}), or ~0.17% of annual emissions from the state of Minnesota, roughly equivalent to the average annual CO_2 emissions from 55,000 personal vehicles (EPA, 2018). This result translates to 2.11 Mg CO_2-eq ha^{-1} yr^{-1}, which is slightly (42%) lower than the estimated per hectare total C loss from a similar study in a UK blanket bog with much higher ditch density (Williamson et al., 2017). Wilson et al. (2016), in a review of drainage and rewetting impacts, estimated CO_2 emissions reduction in rewetted, previously drained boreal forested nutrient-poor peatlands of 2.45 Mg

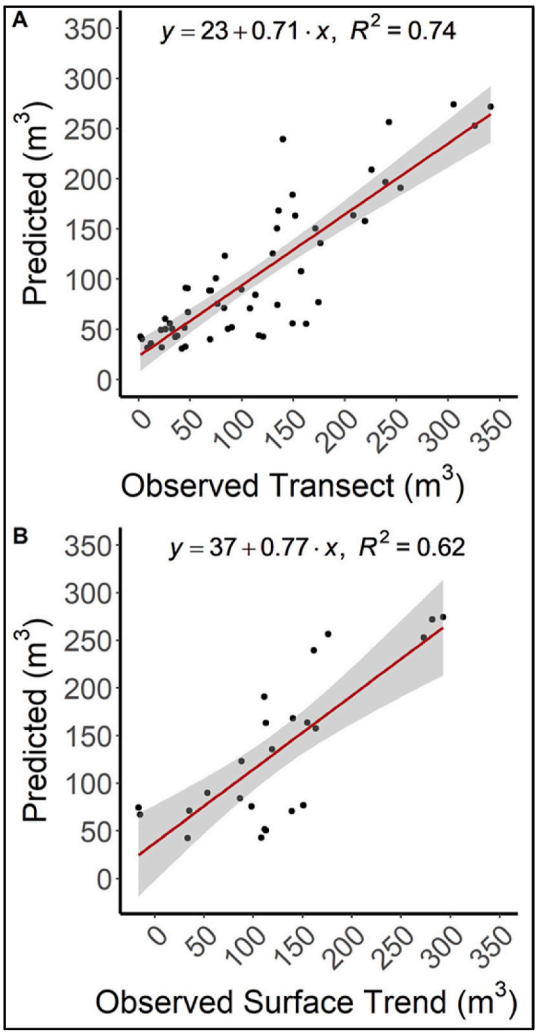

Fig. 4. Volume loss within each AOI between: A) Average AOI transect volume change measured and predicted volume change values derived from the GLMM tree classifications (n = 55); B) Volume change measured in each AOI through the surface trend analysis and predicted volume change values derived from the GLMM tree classifications (n = 24). Units in 1000 m^3.

CO_2-eq $ha^{-1}yr^{-1}$, about 16% higher than our estimate. The convergence of our results with the generalized estimates of Wilson et al. (2016), despite the difference in methods, provides a stronger basis for our C loss calculations.

Although numerous studies have found that peatlands revert to C sinks in the years following peatland restoration (Wilson et al., 2016; Nugent et al., 2018; Günther et al., 2020; Ratcliffe et al., 2020), a number of uncertainties persist, including the dynamics of other GHGs, especially methane (CH_4) and nitrous oxide (N_2O) (Wilson et al., 2016). Methane has a global warming potential (GWP) 28 (without feedbacks to climate) to 34 (with feedbacks to climate) times higher than that of CO_2 (Myhre et al., 2013). Methane emissions decrease with drainage (Glenn et al., 1993; Turetsky et al., 2014), although ditches are themselves hotspots of CH_4 emissions (Minkkinen and Laine, 2006; Green et al., 2018). Conversely, N_2O has a GWP 265 (without feedbacks) to 298 (with feedbacks) times higher than that of CO_2 (Myhre et al., 2013), and increases following drainage, especially from rewetted agricultural fields (Salm et al., 2012; Liu et al., 2020). Incorporating all components of GHG emissions (CO_2, DOC, CH_4, N_2O), the best estimate of rewetting emissions reductions of drained boreal peatlands was 1.21 and 1.57 Mg CO_2-eq ha^{-1} yr^{-1} for nutrient poor and nutrient rich forested peatlands, respectively (Wilson et al., 2016). We need to validate these estimates using studies of GHG emissions in the study region to obtain a more reliable estimate of the climate forcing caused by peatland drainage and rewetting.

4.2. Carbon loss calculations

The oxidative component of peatland subsidence describes the loss of C mass due to increased oxidation rates of organic material in the deeper aerobic layers of peat following drainage (Clymo, 1983; Drexler et al., 2009). Although the fraction of volume loss attributed to C mass loss from peat oxidation can vary widely among peatland ecosystems (Couwenberg et al., 2010), the Pronger et al. (2014) approach used in the present study was based on a synthesis that demonstrated its strong relationship with time since drainage. Because those equations were not explicitly developed for Minnesota, our use of 51% oxidation should be considered provisional, with further research examining the changes in peat bulk density and C content along our transects warranted. It should also be noted that our C loss estimates are partially dependent on average bulk density values, which vary spatially, both horizontally and vertically. In using an average bulk density value for two broad peatland types, we likely overestimate C loss from ditches in which volume loss has occurred primarily in the top 0–25 cm of peat, while underestimating C loss where volume loss has extended into deep peat layers. Despite these uncertainties, our C loss estimates are very similar to estimated annual CO_2–C emissions from drained boreal peatlands described by the Intergovernmental Panel on Climate Change (IPCC, 2013) (Table 5).

While it has been suggested that increased biomass production following water table drawdown can increase peatland C stocks in actively managed forests (Minkkinen and Laine, 1998), partially or fully offsetting the C loss from peat oxidation, we found no evidence of this in our study (Supplementary Materials, S7). Similar results have been found in studies of C balances in drained peatlands in the region (Chimner et al., 2017). This difference is likely attributable to the lack of active forest management, periodic flooding by beavers, spotty ditch maintenance, and low nutrient status, all of which could constrain tree productivity responses to drainage.

4.3. Predictors of volume loss

Many of our hypothesized predictor variables were significantly related to peat volume loss. In particular, as predicted, fibric dysic peatland types displayed a more pronounced volume loss in response to drainage than did the more sapric, euic peatlands. As the water table is lowered the large pores of the less decomposed fibric peat are quickly evacuated of water with an increase in soil tension (Kennedy and Price, 2005), while water held in smaller pores of sapric peat is maintained under equal soil tension. Given the volume reduction potential determined by initial peat matrix pore sizes, it is expected that fibric peat would be more susceptible to volume loss following drainage than would sapric peat; this is a pattern that is borne out in our results (Fig. 2b). Additionally, more fibric dysic *Sphagnum* peat has a high carbohydrate content that, when compared with more sapric euic fen peat, could be more susceptible to decomposition upon drainage (Hodgkins et al., 2018; Verbeke, 2018).

The higher peat volume loss on the downslope side of the ditch was consistent with our hypothesis. Lateral flow of surplus water in a peatland is less constrained in the more permeable acrotelm than in the deeper, compacted catotelm, meaning that the majority of horizontal water movement happens near the peat surface (Damman, 1986). A ditch will intercept water from the upslope side and translocate it through the ditch network, lessening the water inputs to the downslope side. This new flow path both enhances volume loss and limits peatland hydrological services.

It has been found that the proportion of subsidence due to mechanical processes decreases with time and that long-term overall subsidence

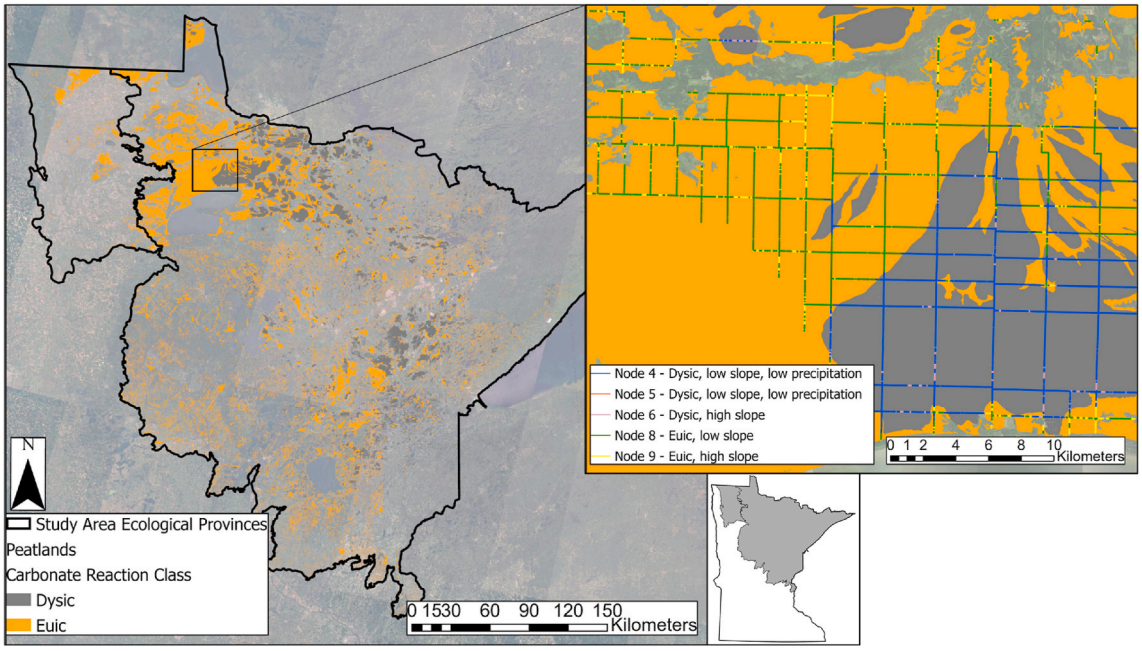

Fig. 5. Map of peatland distribution within the study area. Inset: Ditches color-coded by classification within a terminal node of the GLMM tree. (Graphic created in Arc Pro 2.5.1. Carbonate reaction class graphics were obtained from the SSURGO database. Ecological provinces, composite aerial imagery, and state outline obtained from the Minnesota Geospatial Commons with full attribution in Supplementary Materials, S11). (For interpretation of the references to color in this figure legend, the reader is referred to the Web version of this article.)

Table 4
Average volume loss scaled by total ditch length for each GLMM tree node. Estimates of C loss calculated using volume loss, an assumption of 51% oxidation, average bulk density values, and average C content. C loss per year (±se) assumes constant rate of C loss for 100 years since drainage.

GLMM tree node	Total volume loss (m^3)	Total C loss (Mg)	Mean ditch effect width (km)	C loss (Mg ha^{-1} yr^{-1})
Node 4 - Dysic, low slope, low MAP	31,561,454	628,137	0.35	0.32 ± 0.06
Node 5 - Dysic, low slope, high MAP	28,176,750	560,774	0.43	0.36 ± 0.06
Node 6 - Dysic, high slope	34,855,028	693,686	0.41	0.51 ± 0.09
Node 8 - Euic, low slope	26,086,973	724,930	0.25	0.19 ± 0.04
Node 9 - Euic, high slope	44,619,657	1,239,934	0.31	0.33 ± 0.07

Table 5
C loss estimates based on volume loss, average ditch effect width, average bulk density, dry mass percent C, and years since drainage. Losses from our study are compared with losses estimated in IPCC (IPCC, 2013). CO_2-eq assumes all C is released as CO_2.

Characteristic	Affected area (ha)	Mg C ha^{-1} yr^{-1}	95% Confidence Interval		Mg CO_2-eq ha^{-1} yr^{-1}
Dysic	48,636	0.40	0.15	0.65	1.46
Euic	75,466	0.26	0.10	0.42	0.95
Total	124,102	0.31			1.15
IPCC estimate (*Drained boreal peatlands*)		0.37	−0.11	0.84	1.36

progresses at a linear rate reflective of ongoing peat oxidation (Pronger et al., 2014). This is due to the rapidity with which initial mechanical densification of the peat matrix occurs during the first years after drainage (Pronger et al., 2014) as well as a number of hydrological feedbacks that limit continued structural changes in an altered peatland (Waddington et al., 2015). Thus, the primary driver of continued subsidence in the study area is likely to be oxidation.

4.4. Environmental management implications

Given the interest in identifying strategies for the retention and restoration of C pools and sinks in natural landscapes to mitigate GHG emissions (Griscom et al., 2017), peatland restoration in Minnesota presents itself as an important option to protect these long-term but vulnerable C sinks. One strategy to mitigate this C loss is to restore the natural hydrology of peatlands by blocking or filling drainage ditches (Chimner et al., 2017, 2018). Effective hydrologic restoration raises water tables and restores biogeochemical processes that protect C stores and facilitate continued peat accretion. It has also been shown to restore the hydrological buffer function of surface peat layers, reducing the connectivity of surface water runoff to groundwater (Ahmad et al., 2020). Land managers are encouraged to explore resources that detail restoration strategies, goals, and outcomes relevant to individual sites and management objectives, including but not limited to GHG emissions reduction (Landry and Rochefort, 2012).

Our analysis contributes to the understanding of the effects of legacy drainage features in Minnesota and demonstrates a significant loss of peat volume and C and a potential area for GHG emission mitigation on Minnesota's natural landscapes. While further research is needed to determine local drivers of peatland degradation and the net radiative forcing effect of peatland restoration in Minnesota, the spatially explicit map outputs of this study could be used to help natural resource managers evaluate potential costs and benefits of restoration activities vs the status quo. In particular, restoration project prioritization could include our site-specific estimates of peat volume and C loss with other factors, such as economics, social acceptability, and feasibility, in rankings of potential sites for restoration.

5. Conclusions

Our study confirmed the widespread loss of peat volume caused by thousands of kilometers of ditches in the peatlands of northern Minnesota. These losses almost certainly include a substantial proportion of peat oxidation to CO_2, and as such contribute to historic and ongoing net GHG emissions from the state of Minnesota. In support of hypothesis 1, volumetric losses were greater in acidic, fibric peatlands than in the more humified, less acidic fen peatlands. Hence these acid peatlands would probably present a higher priority target for restoration, all else being equal. In support of hypothesis 2, we found several significant geomorphological and climatic predictors of peat volume loss. Our final decision tree model included geomorphological, biogeochemical, and climatic predictors, indicating the likely dominant controls these factors play in peatland response to ditching. Furthermore, in support of hypothesis 3 we found that downslope peatlands that had been cut off from upslope water sources lose more peat than upslope areas. Restoration that targets re-establishing these flows across ditches could have a large positive impact on peat accumulation in these downslope areas. Our estimates of the ditch-associated loss of C from these peatlands indicate that they are prime targets for hydrologic restoration as part of natural climate solutions, and our map could enhance comprehensive peatland restoration planning tools being developed to assist land managers in developing effective restoration projects.

Declaration of competing interest

The authors declare that they have no known competing financial interests or personal relationships that could have appeared to influence the work reported in this paper.

Acknowledgements

Liam Krause was partially supported by the USDA Forest Service operating funding to EAL, RKK, and ESK. We thank Mike Battaglia for feedback on mapping methods.

Appendix A. Supplementary data

Supplementary data to this article can be found online at https://doi.org/10.1016/j.jenvman.2021.113090.

Credit author statement

Liam Krause: Conceptualization, Methodology, Formal analysis, Investigation, Data curation, Writing – original draft, Writing – review & editing, Visualization, Kevin McCullough: Methodology, Formal analysis, Data curation, Visualization, Evan Kane: Conceptualization, Resources, Writing – review & editing, Supervision, Funding acquisition, Randy Kolka: Methodology, Writing – review & editing, Funding acquisition, Rod Chimner: Methodology, Writing – review & editing, Erik Lilleskov: Conceptualization, Methodology, Resources, Writing – original draft, Writing – review & editing, Supervision, Project administration, Funding acquisition.

References

Ahmad, S., Liu, H., Günther, A., Cowenberg, J., Lennartz, B., 2020. Long-term rewetting of degraded peatlands restores hydrological buffer function. Sci. Total Environ. 749, 141571. https://doi.org/10.1016/j.scitotenv.2020.141571.

Averell, J., McGrew, P., 1929. The Reaction of Swamp Forests to Drainage in Northern Minnesota. Department of Drainage and Waters. State of Minnesota.

Boelter, D., 1968. Important physical properties of peat materials. In: Proceedings of the Third International Peat Congress. Quebec, Canada, pp. 150–154.

Boelter, D., 1972. Water table drawdown around an open ditch in organic soils. J. Hydrol. 15, 329–340.

Bradof, K., 1992. Ditching of the red lake peatland during the homestead era. In: Wright, H., Coffin, B., Aaseng, N. (Eds.), The Patterned Peatlands of Minnesota. University of Minnesota Press, Minneapolis, MN, pp. 263–284.

Braekke, F., 1983. Water table levels at different drainage intensities on deep peat in northern Norway. For. Ecol. Manag. 5, 169–192.

Bridgham, S., Updegraff, K., Pastor, J., 1998. Carbon, nitrogen, and phosphorus mineralization in northern wetlands. Ecology 79, 1445–1561. https://doi.org/10.1890/0012-9658(1998)079[1545:CNAPMI]2.0.CO;2.

Chimner, R., Pypker, T., Hribljan, J., Moore, P., Waddington, J., 2017. Multi-decadal changes in water table levels alter peatland carbon cycling. Ecosystems 20, 1042–1057. https://doi.org/10.1007/s10021-016-0092-x.

Chimner, R., Cooper, D., Bidwell, M., Culpepper, A., Zillich, K., Nydick, K., 2018. A new method for restoring ditches in peatlands: ditch filling with fiber bales. Restor. Ecol. 27, 63–69. https://doi.org/10.1111/rec.12817.

Clymo, R., 1983. Peat. In: Gore, A., Goodall, D. (Eds.), Mires: Swamp, Bog, Fen, and Moor. A General Studies. Elsevier, Amsterdam, pp. 159–224.

Couwenberg, J., Dommain, R., Joosten, H., 2010. Greenhouse gas fluxes from tropical peatlands in south-east Asia. Global Change Biol. 16, 1715–1732. https://doi.org/10.1111/j.1365-2486.2009.02016.x.

Damman, A., 1986. Hydrology, development, and biogeochemistry of ombrogenous peat bogs with special reference to nutrient relocation in a western Newfoundland bog. Can. J. Bot. 64, 384–394.

Drexler, J., Fontaine, C., Deverel, S., 2009. The legacy of wetland drainage on the remaining peat in the Sacramento – san Joaquin Delta, California, USA. Wetlands 29, 372–386.

EPA, 2018. Greenhouse Gas Emissions from a Typical Passenger Vehicle. Office of Transportation and Air Quality. EPA-420-F-18-008.

Fokkema, M., Smits, N., Hothorn, T., Kelderman, H., 2018. Detecting treatment-subgroup interactions in clustered data with generalized linear mixed-effects model trees. Behav. Res. Methods 50, 2016–2034. https://doi.org/10.3758/s13428-017-0971-x.

Fokkema, M., Edbrooke-Childs, J., Wolpert, M., 2020. Generalized linear mixed-model (GLMM) trees: a flexible decision-tree method for multilevel and longitudinal data. Psychother. Res. https://doi.org/10.1080/10503307.2020.1785037.

Glenn, S., Heyes, A., Moore, T., 1993. Carbon dioxide and methane fluxes from drained peat soils, southern Quebec. Global Biogeochem. Cycles 7, 247–257. https://doi.org/10.1029/93GB00469.

Gorham, E., Wright, H., 1979. Ecological and Floristic Studies of the Red Lake Peatland: Final Report to Peat Program. Minnesota Department of Natural Resour. http://purl.umn.edu/151360.

Gorham, E., Janssens, J., Glaser, P., 2003. Rates of peat accumulation during the postglacial period in 32 sites from Alaska to Newfoundland, with special emphasis on northern Minnesota. Can. J. Bot. 81, 429–438.

Green, S., Baird, A., Evans, C., Peacock, M., Holden, J., Chapman, P., Smart, R., 2018. Methane and carbon dioxide fluxes from open and blocked ditches in a blanket bog. Plant Soil 424, 619–638.

Griscom, B., et al., 2017. Natural climate solutions. Proc. Natl. Acad. Sci. Unit. States Am. 114, 11645–11650.

Günther, A., Barthelmes, A., Huth, V., Joosten, H., Jurasinski, G., Koebsch, F., Cowenberg, J., 2020. Prompt rewetting of drained peatlands reduces climate warming despite methane emissions. Nat. Commun. 11, 1644. https://doi.org/10.1038/s41467-020-15499-z.

Hanson, Mark J., 1987. Damming agricultural drainage: the effect of wetland preservation and federal regulation on agricultural drainage in Minnesota. William Mitchell Law Rev. 13, 3. http://open.mitchellhamline.edu/wmlr/vol13/iss1/3.

Hill, B., Jicha, T., Lehto, L., Elonen, C., Sebestyen, S., Kolka, R., 2016. Comparisons of soil nitrogen mass balances for an ombrotrophic bog and minerotrophic fen in northern Minnesota. Sci. Total Environ. 550, 880–892. https://doi.org/10.1016/j.scitotenv.2016.01.178.

Hodgkins, S., Richardson, C., Dommain, R., Wang, H., Glaser, P., Verbeke, B., Winkler, R., Cobb, A., Rich, V., Missilmani, M., Flanagan, N., Ho, M., Hoyt, A., Harvey, C., Vining, S., Hough, M., Moore, T., Richard, P., De La Cruz, F., Toufaily, J., Hamdan, R., Cooper, W., Chanton, J., 2018. Tropical peatland carbon storage linked to global latitudinal trends in peat recalcitrance. Nat. Commun. 9, 3640. https://doi.org/10.1038/s41467-018-06050-2.

Hooijer, A., Page, S., Jauhiainen, J., Lee, W., Lu, X., Idris, A., Anshari, G., 2012. Subsidence and carbon loss in drained tropical peatlands. Biogeosciences 9, 1053–1071. https://doi.org/10.5194/bg-9-1053-2012.

Hothorn, T., Hornik, K., Zeilis, A., 2006. Unbiased recursive partitioning: a conditional inference framework. J. Comput. Graph Stat. 15, 651–674. https://doi.org/10.1198/106186006X133933.

IPCC, 2013. In: Hiraishi, T., Krug, T., Tanabe, K., Srivastava, N., Baasansuren, J., Fukuda, M., Troxler, T. (Eds.), Supplement to the 2006 IPCC Guidelines for National Greenhouse Gas Inventories: Wetlands. Published: IPCC, Switzerland.

Kaat, A., Joosten, H., 2008. Factbook for UNFCCC Policies on Peat Carbon Emissions. Wetlands International, Wageningen, The Netherlands.

Kennedy, G., Price, J., 2005. A conceptual model of volume-change controls on the hydrology of cutover peats. J. Hydrol. 302, 13–27. https://doi.org/10.1016/j.jhydrol.2004.06.024.

Kloiber, S., Norris, D., Bergman, A., 2019. Minnesota Wetland Inventory: User Guide and Summary Statistics. Minnesota Department of Natural Resources, St. Paul, MN.

Kolka, R., Bridgham, S., Ping, C., 2016. Soils of peatlands: histosols and gelisols. In: Vepraskas, M., Craft, C. (Eds.), Wetland Soils: Genesis, Hydrology, Landscapes, and Classification II. Taylor and Francis Group, Boca Raton, pp. 277–309. https://doi.org/10.1201/b18996.

Kolka, R., Trettin, C., Tang, W., Krauss, K., Bansal, S., Drexler, J., Wickland, K., Chimner, R., Hogan, D., Pindilli, E., Benscoter, B., Tangen, B., Kane, E., Bridgham, S.,

Richardson, C., 2018. Chapter 13: terrestrial wetlands. In: Cavallaro, N., Shrestha, G., Birdsey, R., Mayes, M., Najjar, R., Reed, S., Romero-Lankao, P., Zhu, Z. (Eds.), Second State of the Carbon Cycle Report (SOCCR2): A Sustained Assessment Report. U.S. Global Change Research Program, Washington, DC, USA, pp. 507–567. https://doi.org/10.7930/SOCCR2.2018.Ch13.

Landry, J., Rochefort, L., 2012. The Drainage of Peatlands: Impacts and Rewetting Techniques. Peatland Ecology Research Group, Université Laval, Québec, Québec, Canada.

Leifeld, J., Wüst-Galley, C., Page, S., 2019. Intact and managed peatland soils as a source and sink of GHGs from 1850 to 2100. Nat. Clim. Change 945–947. https://doi.org/10.1038/s41558-019-0615-5.

Liu, H., Wrange-Mönnig, N., Lennartz, B., 2020. Rewetting strategies to reduce nitrous oxide emissions from European peatlands. Nat. Commun. Earth and Environ. 1, 17. https://doi.org/10.1038/s43247-020-00017-2.

Loisel, J., Gallego-Sala, A., Amesbury, M., Magnan, G., Anshari, G., Beilman, D., Benavides, J., Blewett, J., Camill, P., Charman, D., Chawchai, S., Hedgpeth, A., Kleinen, T., Korhola, A., Large, D., Mansilla, C., Müller, J., van Bellen, S., West, J., Yu, Z., Bubier, J., Garneau, M., Moore, T., Sannel, A., Page, S., Väliranta, M., Bechtold, M., Brovkin, V., Cole, L., Chanton, J., Christensen, T., Davies, M., Vleeschouwer, F., Finkelstein, S., Frolking, S., Gałka, M., Gandois, L., Girkin, N., Harris, L., Heinemeyer, A., Hoyt, A., Jones, M., Joos, F., Juutinene, S., Kaiser, K., Lacourse, T., Lamentowicz≤, M., Larmola, T., Leifeld, J., Lohila, A., Milner, A., Minkkinen, K., Moss, P., Naafs, B., Nichols, J., O'Donnell, J., Payne, R., Philben, M., Piilo, S., Quillet, A., Ratnayake, A., Roland, T., Sjögersten, S., Sonnetag, O., Swindels, G., Swinnen, W., Talbot, J., Treat, C., Valach, A., Wu, J., 2020. Expert assessment of future vulnerability of the global peatland carbon sink. Nat. Clim. 11, 70–77. https://doi.org/10.1038/s41558-020-00944-0.

McFarlane, K., Hanson, P., Iversen, C., Phillips, J., Brice, D., 2018. Local spatial heterogeneity of Holocene carbon accumulation throughout the peat profile of an ombrotrophic Northern Minnesota bog. Radiocarbon 60, 941–962.

Minkkinen, K., Laine, J., 1998. Long-term effect of forest drainage on the peat carbon stores of pine mires in Finland. Can. J. For. Res. 28, 1267–1275.

Minkkinen, K., Laine, J., 2006. Vegetation heterogeneity and ditches create spatial variability in methane fluxes from peatlands drained for forestry. Plant Soil 285, 289–304.

Minnesota Department of Natural Resources, 1984. Recommendations for the Protection of Ecologically Significant Peatlands in Minnesota. Minnesota Department of Natural Resources, St. Paul.

Minnesota Department of Natural Resources, 1987. The Minnesota Peat Program Summary Report 1981-1986. Minnesota Department of Natural Resources, St. Paul.

Minnesota Department of Natural Resources, 2003. Field Guide to the Native Plant Communities of Minnesota: the Laurentian Mixed Forest Province. State of Minnesota. Department of Natural Resources.

Minnesota Department of Natural Resources, 2005a. Field Guide to the Native Plant Communities of Minnesota: Prairie Parkland and Tallgrass Aspen Parklands Provinces. State of Minnesota, Department of Natural Resources.

Minnesota Department of Natural Resources, 2005b. Field Guide to the Native Plant Communities of Minnesota: Eastern Broadleaf Forest Province. State of Minnesota. Department of Natural Resources.

Minnesota Department of Natural Resources, 2007. Peat Inventory of Minnesota. State of Minnesota, Department of Natural Resources. https://gisdata.mn.gov/nl/dataset/geos-peat-inventory.

Minnesota Department of Natural Resources, 2014. MN Topo Help: Revolutionizing the Way We Look at Minnesota's Landscape. Minnesota Department of Natural Resources. http://files.dnr.state.mn.us/aboutdnr/gis/mntopo/mntopo_help_document.pdf. (Accessed 15 October 2019).

Minnesota Department of Natural Resources, 2016. Buffer Protection Map, Minnesota. State of Minnesota, Department of Natural Resources, Ecological and Water Resources Division. https://gisdata.mn.gov/dataset/env-buffer-protection-mn.

Minnesota Department of Natural Resources, 2017. LiDAR Elevation Data for Minnesota. Minnesota IT Service. Geospatial Information Office. https://www.mngeo.state.mn.us/chouse/elevation/lidar.html.

Minnesota Department of Natural Resources, 2019. National Wetland Inventory for Minnesota. State of Minnesota Department of Natural Resources. https://gisdata.mn.gov/dataset/water-nat-wetlands-inv-2009-2014.

Minnesota Pollution Control Agency, 2019. Greenhouse Gas Emissions in Minnesota: 1990-2016. State of Minnesota. Minnesota Pollution Control Agency accessed. https://www.pca.state.mn.us/sites/default/files/lraq-2sy19.pdf. (Accessed 14 December 2020).

Moore, P., Bellamy, D., 1974. Peatlands. Springer-Verlag, New York, New York, USA.

Myhre, G., Shindell, D., Bréon, F., Collins, W., Fuglestvedt, J., Huang, J., Koch, D., Lamarque, J., Lee, D., Mendoza, B., Nakajima, T., Robock, A., Stephens, G., Takemura, T., Zhang, H., 2013. Anthropogenic and natural radiative forcing. In: Stocker, T., Qin, D., Plattner, G., Tignor, M., Allen, S., Boschung, J., Nauels, A., Xia, Y., Bex, V., Midgley, P. (Eds.), Climate Change 2013: the Physical Science Basis. Contribution of Working Group I to the Fifth Assessment Report of the Intergovernmental Panel on Climate Change. Cambridge University Press, Cambridge, United Kingdom and New York, NY, USA.

Nugent, K., Strachan, I., Strack, M., Roulet, N., Rochefort, L., 2018. Multi-year net ecosystem carbon balance of a restored peatland reveals a return to carbon sink. Global Change Biol. 24, 5751–5768. https://doi.org/10.1111/gcb.14449.

Page, S., Baird, A., 2016. Peatlands and global climate change: response and resilience. Annu. Rev. Environ. Resour. 41, 35–57.

PRISM, 2019. PRISM Climate Group. Oregon State University. http://prism.oregonstate.edu.

Pronger, J., Schipper, L., Hill, R., Campbell, D., McLeod, M., 2014. Subsidence rates of drained agriculture peatlands in New Zealand and the relationship with time since drainage. J. Environ. Qual. 43, 1442–1449. https://doi.org/10.2134/jeq2013.12.0505.

Rezanezhad, F., Price, J., Quinton, W., Lennartz, B., Milojevic, T., Van Cappellen, P., 2016. Structure of peat soils and implication for water storage, flow and solute transport: a review update for geochemists. Chem. Geol. 429, 75–84. https://doi.org/10.1016/j.chemgeo.2016.03.010.

R Core Team, 2020. R: A Language and Environment for Statistical Computing. Vienna, Austria. Available at: https://www.R-project.org/.

Ratcliffe, J., Campbell, D., Schipper, L., Wall, A., Clarkson, B., 2020. Recovery of the CO_2 sink in a remnant peatland following water table lowering. Sci. Total Environ. 718, 134613. https://doi.org/10.1016/j.scitotenv.2019.134613.

Salm, J., Maddison, M., Tammik, S., Soosaar, K., Truu, J., Mander, Ü., 2012. Emissions of CO_2, CH_4 and N_2O from undisturbed, drained and mined peatlands in Estonia. Hydrobiologia 692, 41–55. https://doi.org/10.1007/s10750-011-0934-7.

SSURGO, 2019. Soil Survey Geographic (SSURGO) Database for Minnesota. https://gisdata.mn.gov/dataset/geos-gssurgo.

Stewart, A., Lance, A., 1991. Effects of moor-draining on the hydrology and vegetation of Northern Pennine blanket bog. J. Appl. Ecol. 28, 1105–1117.

Trabucco, A., Zomer, R., 2019. Global High-Resolution Soil-Water Balance. figshare. https://doi.org/10.6084/m9.figshare.7707605.v3.

Turetsky, M., Kotowska, A., Bubier, J., Dise, N., Crill, P., Hornibrook, E., Minkkinen, K., Moore, T., Myers-Smith, I., Nykänen, H., Olefeldt, D., Rinne, J., Saarnio, S., Shurpali, N., Tuittila, E., Waddington, J., White, J., Wickland, K., Wilmking, M., 2014. A synthesis of methane emissions from 71 northern, temperate, and subtropical wetlands. Global Change Biol. 20, 2183–2197. https://doi.org/10.1111/gcb.12580.

Verbeke, B., 2018. Peatland Organic Matter Chemistry Trends over a Global Latitudinal Gradient. Doctoral dissertation, The Florida State University.

Waddington, J., Morris, P., Ketteridge, N., Thompson, D., Moore, P., 2015. Hydrological feedbacks in northern peatlands. Ecohydrology 8, 113–127. https://doi.org/10.1002/eco.1493.

Williamson, J., Rowe, E., Reed, D., Ruffino, L., Jones, P., Dolan, R., Buckingham, H., Norris, D., Astbury, S., Evans, C., 2017. Historical peat loss explains limited short-term response of drained blanket bogs to rewetting. J. Environ. Manag. 188, 278–286. https://doi.org/10.1016/j.jenvman.2016.12.018.

Wilson, B., 2016. History of Drainage in the Northern Midwestern US. University of Minnesota accessed. https://extension.umn.edu/crop-production/agricultural-drainage#history-1358164. (Accessed 10 July 2020).

Wilson, D., Blain, D., Couwenberg, J., Evans, C., Murdiyarso, D., Page, S., Renou-Wilson, F., Rieley, J., Sirin, A., Strack, M., Tuittila, E., 2016. Greenhouse gas emission factors associated with rewetting of organic soils. Mires Peat 17, 1–28. https://doi.org/10.19189/MaP.2016.OMB.222.

Xu, J., Morris, P., Liu, J., Holden, J., 2018. Peatmap: refining estimates of global peatland distribution based on a meta-analysis. Catena 160, 134–140. https://doi.org/10.1016/j.catena.2017.09.010.